Acc. Chem. Res. **2004,** *37,* 421−429

ARTICLES

Reactions of the Diiron Enzyme Stearoyl-Acyl Carrier Protein Desaturase

BRIAN G. FOX,* KAREN S. LYLE, AND CORINA E. ROGGE

Department of Biochemistry, College of Agricultural and Life Sciences, University of Wisconsin, Madison, Wisconsin 53706

Received December 2, 2003

ABSTRACT

Stearoyl-acyl carrier protein Δ^9 desaturase (Δ9D) produces oleic acid, a nutritionally valuable fatty acid containing a cis double bond between C-9 and C-10. This multiprotein diiron enzyme complex reacts with stearoyl-acyl carrier protein, reduced [2Fe−2S] ferredoxin, and O_2 to complete the highly regiospecific and stereoselective desaturation reaction. Interactions with the acyl chain provide stability to the enzyme−substrate complex, give an energetic contribution to catalytic selectivity, and help to order the electron transfer, O_2 binding, and C−H bond cleavage steps of catalysis. Reactions with natural acyl chains indicate the involvement of a highly reactive diiron intermediate capable of oxidizing secondary C−H bonds (bond dissociation energy ≈ 95 kcal/mol), but also capable of diagnostic O-atom transfer reactions with the appropriate substrate analogues. For soluble Δ9D, the natural reaction may initiate at the C-10 position, in contrast to the well-established initial reactivity of the membrane enzyme homologue stearoyl-coenzyme A (CoA) Δ^9 desaturase at the C-9 position.

Importance of Fatty Acid Desaturases

Figure 1 shows a representative reaction catalyzed by the fatty acid desaturase enzymes. These iron-containing multiprotein complexes are used to insert double bonds into fatty acyl chains after their biosynthesis.[1−3] Desaturases provide lipid precursors to cell membranes, to nutritionally essential polyunsaturated fatty acids, to prostaglandins,[4] and to the plant "wound-response" hormone jasmonic acid.[5] Diseases associated with abnormal lipid metabolism include obesity, non-insulin-dependent diabetes, hypertension, cardiovascular disorders, immune distress, neurological pathologies, and many others. Unsaturated fatty acids also have substantial commercial value and offer promise as renewable carbon precursors for green-based industries.[6]

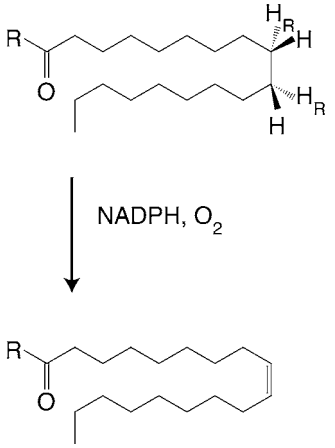

FIGURE 1. Reactants and products of a representative fatty acid desaturase reaction. This is a $2e^-$ and O_2-dependent α,β-dehydrogenation at an unactivated position of the fatty acyl chain resulting in cis double bond formation. For integral membrane stearoyl-CoA Δ^9 desaturase, R is coenzyme A; for soluble stearoyl-ACP Δ^9 desaturase, R is holo-ACP.

Despite the obvious importance of unsaturated fatty acids, many details of desaturase catalysis are poorly understood, including the contributions of protein interactions, the reactivity of the required diiron centers, and the nature of substrate intermediates. The long-term goal of our research is to provide a more complete understanding of these essential catalytic mechanisms by study of representative soluble and integral membrane desaturases.

Integral Membrane Desaturases

Mammals and other eukaryotes contain integral membrane desaturases.[1] This superfamily also includes hydroxylases,[7] epoxygenases, and acetylenases.[8] Membrane desaturases are identified by an eight histidine motif that may provide ligands to the catalytically essential diiron center.[9] Membrane desaturases react with acyl chains attached to different polar headgroups including coenzyme A (CoA), diacyl glycerol, or phospholipids.[1] Excellent reviews of the phylogeny,[1] catalysis,[10] and physiology[11] of the membrane desaturases are available.

Soluble Acyl-ACP Desaturases

Presently, only plants are known to contain soluble acyl-acyl carrier protein (ACP) desaturases. They are members

Brian G. Fox received a B.A. in Chemistry from Carleton College with inspiration from Prof. J. Mohrig, a Ph.D. in Biochemistry from the University of Minnesota under the guidance of Prof. J. D. Lipscomb, and a postdoctoral education from Prof. E. Münck at Carnegie Mellon University. He joined the University of Wisconsin Department of Biochemistry in 1993. His major research interest is studying mechanisms of enzyme action.

Karen S. Lyle received a B.S. in Chemistry from Arizona State University and a Ph.D. in Biochemistry at the University of Wisconsin in 2003.

Corina E. Rogge received a B.A. in Chemistry from Bryn Mawr College and a Ph.D. in Chemistry from the Yale University under the supervision of Prof. J. Caradonna. After postdoctoral work at the University of Wisconsin, she moved to the Department of Internal Medicine at the University of Texas Medical Center at Houston to continue postdoctoral studies with Prof. R. Kulmacz.

* Corresponding author. Mailing address: Department of Biochemistry, 141B Biochemistry Addition, 435 Babcock Drive, University of Wisconsin, Madison, WI 53706. E-mail: bgfox@biochem.wisc.edu. Telephone: (608) 262-9708. Fax: (608) 262-3453.

10.1021/ar030186h CCC: $27.50 © 2004 American Chemical Society
Published on Web 05/29/2004

of a superfamily of diiron enzymes including ribonucleotide diphosphate reductase and bacterial hydroxylases.[12,13] Through study of these enzymes, the diiron center has been recognized as a ubiquitous, potent, and versatile oxidation catalyst. This realization has generated significant interest in their biochemistry,[14,15] structure,[16−19] and applications.[3,20] In this work, we focus on the reactivity of the best-characterized soluble desaturase, stearoyl-ACP Δ^9 desaturase (Δ9D) and the preferred substrate, acyl-acyl carrier protein (acyl-ACP).

Acyl-Acyl Carrier Protein. The physiologically relevant substrates of Δ9D are acyl-ACPs. Acyl-ACPs are small, highly soluble proteins used for lipid biosynthesis, cell wall biosynthesis, nonribosomal peptide synthesis, autoinducer biosynthesis, and other reactions in plants and bacteria. An ACP is initially expressed as an inactive apo-protein that undergoes posttranslational modification in a CoA-dependent reaction catalyzed by holo-[ACP] synthase (EC 2.7.8.7), yielding holo-ACP.[21] For the studies described below, purified holo-ACP was acylated using 2-acylglycerophosphoethanolamine acyltransferase [EC 6.2.1.20, acyl-[ACP] synthetase[22]], which catalyzes ATP-dependent thioester bond formation in a nonphysiological in vitro reaction.

Δ9D Structure. Figure 2 shows the four proteins required for soluble desaturase activity. Reducing equivalents from NADPH are transferred from ferredoxin reductase (FdR) to ferredoxin (Fd) and then to stearoyl-ACP Δ^9 desaturase (Δ9D). In the presence of O_2, the 9*R*,10*R* hydrogen atoms of stearoyl-ACP (18:0-ACP) are removed to give oleoyl-ACP (*cis*-Δ^9-18:1-ACP) with complete fidelity of double bond position and cis stereochemistry (18:0 designates an eighteen carbon fatty acid with no double bonds; *cis*-Δ^9-18:1 is an eighteen carbon fatty acid with a cis double bond starting at the C-9 position).[10] Upon consideration of the fate of O_2, this is an oxidase reaction, since it converts O_2 into 2 mol of water, $O_2 + 4e^- + 4H^+ \rightarrow 2H_2O$.

A 2.4 Å structure shows that Δ9D is a homodimer (Figure 2).[17] The central α helical bundle that provides the conserved metal binding motif of glutamate and histidine residues[10] has high structural similarity to ribonucleotide reductase.[16] In Δ9D, the diiron center is buried alongside a bent channel, presumably at the correct depth from the surface to position C-9 and C-10 of the 18:0 moiety of 18:0-ACP for reaction. Since acyl-ACPs are the only relevant substrates of Δ9D,[23−25] many unique aspects of catalysis arise from influence of extensive enzyme−substrate interactions.

The assignment of the substrate channel is supported by mutagenesis,[26] which revealed that the T117R/G188L mutations (lying near the end of the substrate binding channel) gave an ∼35-fold shift in acyl chain selectivity from 18:0-ACP toward 16:0-ACP. This work and comparable results on other diiron enzymes[27−29] extend the promise of the manipulation of diiron enzyme active sites to achieve new catalytic outcomes while maintaining an overall favorable k_{cat} and k_{cat}/K_M during an exceedingly complex reaction cycle.

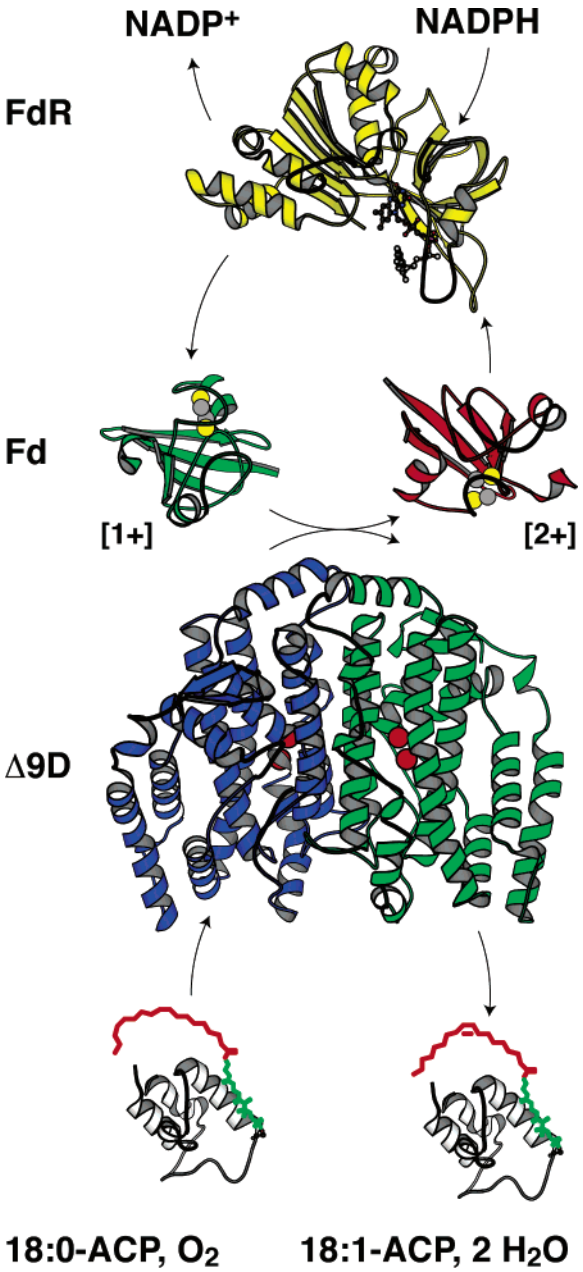

FIGURE 2. The Δ9D complex consists of ferredoxin reductase (FdR, PDB code 1FNB), [2Fe−2S] ferredoxin (Fd, 1FXA), stearoyl-ACP Δ^9 desaturase (Δ9D, 1AFR), and 18:0-ACP (1ACP). The phosphopantetheine and acyl chain of 18:0-ACP and *cis*-Δ^9-18:1-ACP are not structurally defined but are added for illustration.

Protein and Acyl Chain Interactions

Biophysical, catalytic, and kinetic approaches have been used to characterize complexes of acyl-ACP and Δ9D. These studies have permitted assembly of an initial model for the catalytic cycle accounting for binding affinities and the order of interactions between Δ9D, 18:0-ACP, and reduced Fd.

Resting Enzyme−Substrate Complex. To investigate binding interactions, the single tyrosine present in *Escherichia coli* ACP, Tyr71, was first converted to *meta*-amino-Tyr71.[21] The aromatic amine was reacted with an acid chloride fluorophore and the apo-fluorophore-ACP was recovered in ∼30% yield. After in vitro phosphopan-

tetheinylation and acylation, 18:0-dansyl-ACP had k_{cat} = 22 min^{-1} and K_M = 2.7 μM, comparable to the unlabeled substrate. Thus the labeled-ACPs provided a catalytically competent probe for studying binding interactions.

Fluorescence anisotropy is a powerful method for studying binding interactions.[30] Anisotropy (r) is calculated from the intensity of vertical and horizontal emission measured from a fluorescent sample excited with vertically polarized light, where $r = (I_{horizontal} - I_{vertical})/(I_{horizontal} + 2I_{vertical})$. At constant viscosity and temperature, anisotropy is proportional to the rotational relaxation time of the fluorophore. Under appropriate circumstances, titration of a small, fluorescently labeled ligand (e.g., acyl-fluorophore-ACP) with a larger, unlabeled binding protein (e.g., Δ9D) gives a change from the low anisotropy of the rapidly rotating small molecule to the increased anisotropy of the more slowly rotating larger complex.

Using dansyl- and fluoresceinyl-labeled 16:0-, 17:0-, and 18:0-ACPs, fluorescence anisotropy was used to study the enzyme−substrate complex.[31] Since Δ9D is a homodimer, the binding of either one or two acyl-ACP molecules was possible with equilibrium constants K_{D1} and K_{D2}. Figure 3A shows that 1 nM 18:0-fluoresceinyl-ACP was tightly bound upon addition of Δ9D (K_{D1} = 13 ± 3 nM) and that an ~4-fold increase in K_{D1} per methylene group occurred upon shortening the acyl chain. In different experiments with 850 nM 18:0-dansyl-ACP, binding to the second subunit of resting Δ9D was estimated to have $K_{D2} \approx 350 \pm 40$ nM. These measurements indicate a weak negative cooperativity for binding of 18:0-ACP to dimeric Δ9D, perhaps mediated by conformational changes introduced from the predicted extensive interactions of the enzyme−substrate complex.

Chain Length Selectivity. Figure 3B shows a stopped-flow anisotropy measurement of k_{off} for reversal of the preformed complex of 18:0-fluoresceinyl-ACP and Δ9D by competition with unlabeled 18:0-ACP. The k_{off}-values depended on acyl-chain length and increased 130-fold for 16:0-ACP (130 s^{-1}) relative to 18:0-ACP (1 s^{-1}). Thus the ~100-fold chain length selectivity for 18:0-ACP versus 16:0-ACP derives in part from partition between nonproductive breakdown of the enzyme−substrate complex (k_{off}) and subsequent steps in catalysis (k_{cat}), including electron transfer, O_2 binding, and chemical steps of double bond insertion.

Figure 4 shows a correspondence between acyl chain length and catalytic selectivity of the Δ9D reaction,[24] where the plot of log(k_{cat}/K_M) versus acyl chain length represents a hydrophobic partitioning equilibrium. In this case, the slope suggested that ~3.5 kJ/mol could be obtained from each methylene group added to the enzyme−substrate complex from 14:0 to 19:0, ~14 kJ/mol total. One plausible use of this binding energy would be to position the substrate in a near-attack configuration,[32] the alignment of the 9*R*,10*R* hydrogen atoms for reaction with the activated diiron center. Notably, the formation of eclipsed methylene hydrogen atoms demanded by the stereochemistry of the desaturation reaction[33] corresponds to ~18 kJ/mol (Figure 4).

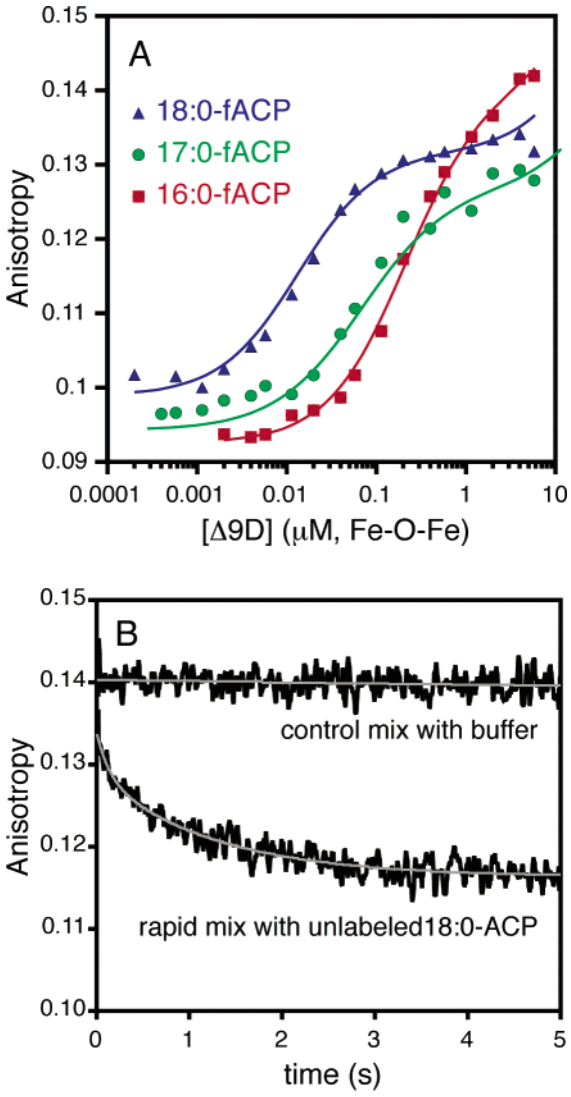

FIGURE 3. Acyl chain length controls the affinity of acyl-ACP for Δ9D:[31] (A) correlation of acyl chain length with K_{D1} as determined by fluorescence anisotropy; (B) determination of k_{off} for 18:0-ACP by using stopped-flow fluorescence anisotropy.

Reactions of the Diiron Center

Spectroscopic methods have played a prominent role in studies of diiron enzymes due to their exquisite sensitivity to changes in electronic configuration at metal centers.[14,18,19] An operational paradigm for diiron enzyme reactivity is that changes in coordination geometry, promoted by protein−protein interactions and by changes in redox state, help to trigger the reaction with O_2 as part of an ordered catalytic cycle.

Figure 5 shows coordination geometries assigned for four different Δ9D redox states and the corresponding resonance Raman and Mössbauer spectra. Resting Δ9D contains diferric centers and has λ_{max} around 350 nm arising from μ-oxo → Fe^{3+} charge transfer.[12] Resonance Raman studies (Figure 5A) of resting Δ9D showed symmetric (ν_s = 519 cm^{-1}) and antisymmetric (ν_{as} = 747 cm^{-1}) vibrational modes of the Fe−O−Fe center. These vibrations shifted in frequency when the enzyme was incubated in $^{18}OH_2$-enriched water, showing that the bridging oxo

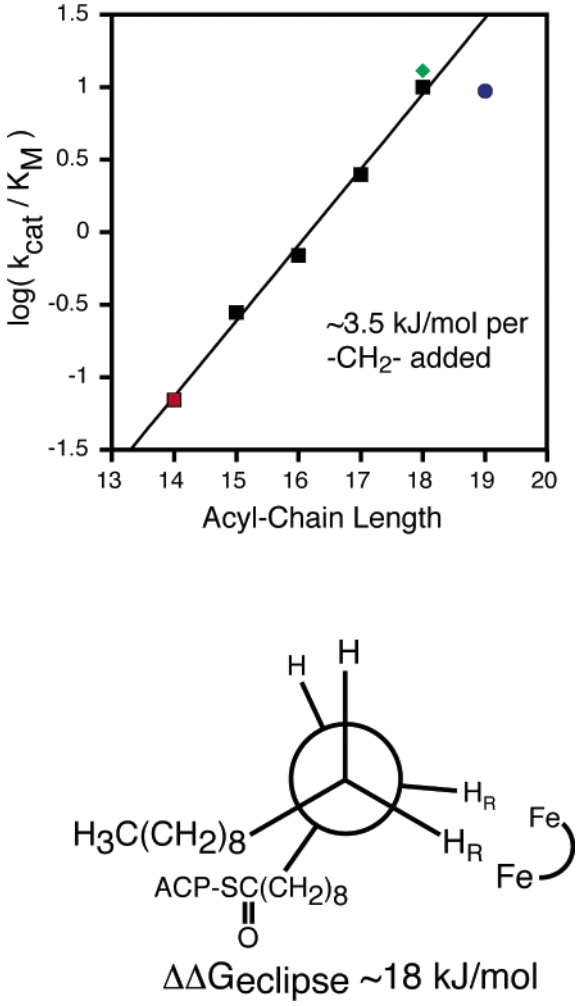

FIGURE 4. Correlation of energy derived from acyl chain binding and conformation required for stereoselectivity[10] of Δ9D catalysis.[24]

position exchanged with solvent ($t_{1/2} \approx 8$ min). Extended X-ray absorption fine structure (EXAFS) and Mössbauer studies of resting Δ9D showed that both oxo- and hydroxo-bridged diiron centers were present (oxo, $\Delta E_{Q1} = 1.53$ mm/s, $\delta_1 = 0.54$ mm/s, 72%; hydroxo, $\Delta E_{Q2} = 0.72$ mm/s, $\delta_2 = 0.49$ mm/s, 21%) with Fe−Fe distances of 3.1 and 3.4 Å, respectively.[34,35]

Treatment of resting Δ9D with sodium dithionite gave a reduced state called 4e⁻ Δ9D (2e⁻ per diiron center) with Mössbauer parameters typical of high-spin ferrous sites ($\Delta E_{Q1} \approx 3.30$ mm/s, $\delta_1 \approx 1.27$ mm/s; $\Delta E_{Q2} \approx 3.05$ mm/s, $\delta_2 \approx 1.28$ mm/s; Figure 5C).[36] Addition of 18:0-ACP gave minor changes in these parameters. Magnetic circular dichroism (MCD) analysis indicated that 4e⁻ Δ9D contained two diiron centers made from two equivalent 5-coordinate iron sites,[37] as in the 2.4 Å structure of photoreduced Δ9D.[17] Upon addition of 18:0-ACP, MCD showed that each diiron center assumed a mixed 4- and 5-coordinate state. This appearance of a 4-coordinate site was proposed to promote binding of O_2.[38]

Upon addition of O_2 to 4e⁻ Δ9D and 18:0-ACP, a bright blue complex was formed with apparent first-order rate of 87 s^{-1}.[23] Resonance Raman and Mössbauer studies revealed that this was a μ-1,2-peroxo-bridged diferric

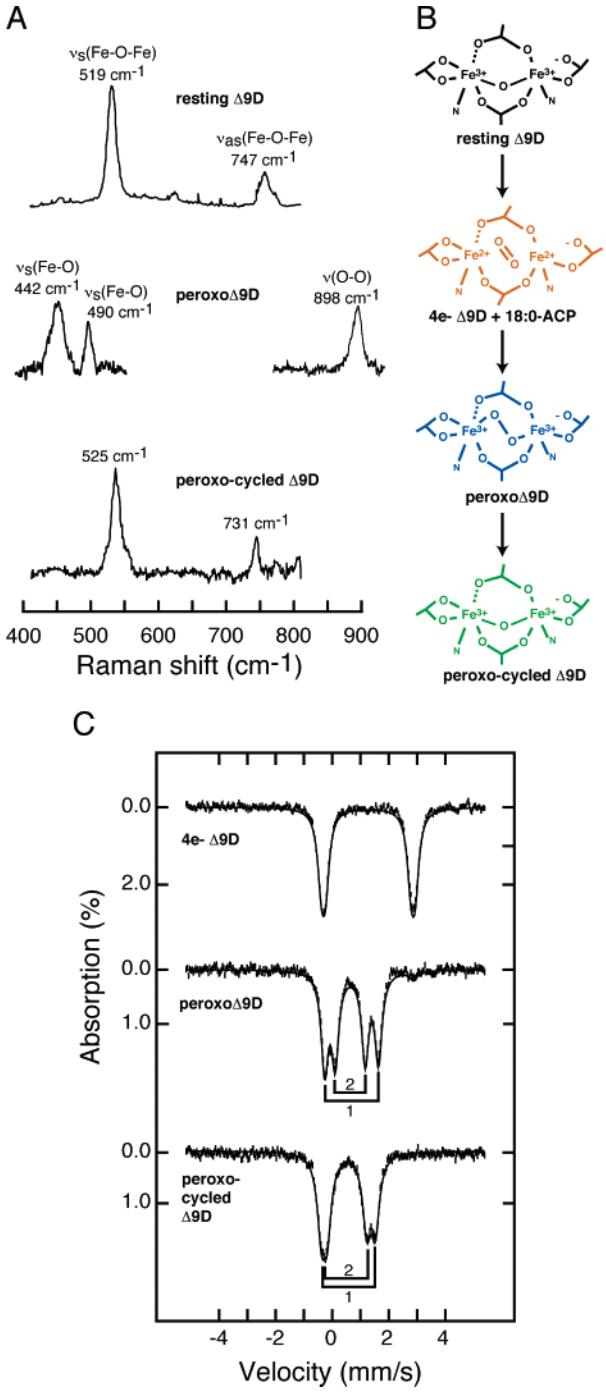

FIGURE 5. Spectroscopic studies of four redox states of Δ9D: (A) resonance Raman;[23] (B) coordination geometries proposed for various states of the diiron center discussed in the text; (C) Mössbauer spectroscopy.[36]

complex, designated peroxoΔ9D (Figure 5). Similar μ-1,2-peroxo-bridged diferric complexes have been observed in all soluble diiron enzymes, and this complex is thought to be an immediate precursor to O−O bond cleavage required to generate the high-valent diferryl species (Fe^{4+}−Fe^{4+}) used for catalysis.[39]

PeroxoΔ9D is unique in three ways, however. First it is remarkably stable with a $t_{1/2}$ for decay of ~30 min at room temperature. Second, the decay proceeds by an oxidase reaction that returns the enzyme to a diferric state

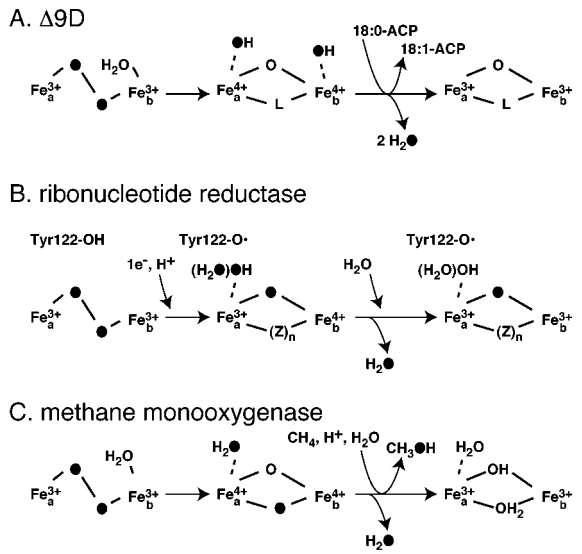

FIGURE 6. Summary of the fate of O_2 during the turnover of diiron enzymes:[40] (A) Δ9D does not incorporate an O-atom from O_2 into the μ-oxo bridge during single-turnover catalysis; (B) ribonucleotide reductase does incorporate an O-atom from O_2 into the μ-oxo bridge during single turnover; (C) methane monooxygenase incorporates an O-atom from O_2 into the hydrocarbon substrate. Incorporation of an O-atom into the μ-oxo bridge could not be determined.

called peroxo-cycled Δ9D (Figure 5) without double bond insertion. The oxidase reaction has no effect on subsequent desaturase activity upon reconstitution with the biological electron-transfer chain. Third, photolysis of peroxoΔ9D at 4.2 K in the Mössbauer instrument gave a diferrous state distinct from $4e^-$ Δ9D, possibly representing the mixed 4- and 5-coordinate diferrous state proposed to be involved in O_2 binding by MCD studies.[37] When the photolyzed sample was warmed to ~77 K, peroxoΔ9D was quantitatively recovered, indicating that the dissociated O_2 was retained in a thermodynamic well within the active site. Factors contributing to the remarkable stability of peroxoΔ9D are not known.

Fate of O_2 after Reaction. Figure 6 summarizes experiments on the fate of O-atoms derived from isotopically labeled O_2 during three major reactions of the diiron enzyme superfamily. These represent endpoints from reaction of related peroxodiferric intermediates. After reduction of Δ9D with reduced [2Fe-2S] Fd and exposure to $^{18}O_2$, 18:1-ACP was formed more rapidly than exchange of the μ-oxo position in the resting Δ9D. Resonance Raman measurements made on these samples showed no incorporation of an ^{18}O atom into the μ-oxo bridge position,[40] suggesting that both O-atoms from O_2 were rapidly lost to solvent during the desaturation reaction. Figure 6A shows a plausible mechanism that would permit the loss of both O-atoms from O_2 as water.

The Δ9D results are distinct from those with ribonucleotide reductase, where resonance Raman[41] and ^{17}O-electron nuclear double resonance (ENDOR)[42] studies showed that an O-atom from O_2 was incorporated into the μ-oxo position upon single-turnover formation of the Tyr122 radical. Moreover, high-fidelity O-atom transfers are known during the hydroxylation reactions of methane monooxygenase[43] and toluene 4-monooxygenase,[40] an outcome that is normally not observed during desaturation by Δ9D. These comparative results provide evidence for the versatility of diiron enzymes and indicate that the details of O_2 activation for these three enzymes are different, despite the substantial number of similar physical and structural properties.

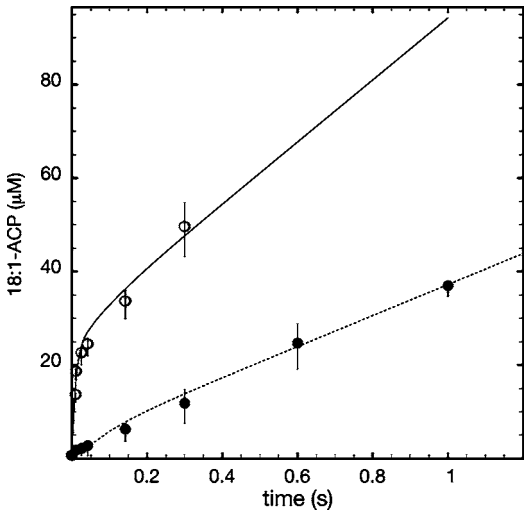

FIGURE 7. Rapid-mix, chemical quench studies:[25] (○) product formation from rapid-mix, chemical quench reactions of the prereduced (treated with reduced Fd) enzyme−substrate complex with aerobic buffer; (●) product formation from reactions of the aerobic enzyme−substrate complex with reduced Fd. The solid lines were calculated by numerical integration using the kinetic model shown in Figure 8.

Transient Kinetics of Reaction

Two different initial conditions have been used for rapid-mix and chemical quench studies of Δ9D: (1) rapid mix of the enzyme−substrate complex prereduced by Fd with aerobic buffer and (2) rapid mix of the oxidized, aerobic enzyme−substrate complex with reduced Fd.[25] In the first case, reaction with O_2 alone is required to initiate the chemical steps of the reaction. In the second case, both electron transfer and reaction with O_2 are required.

Several distinct aspects of the Δ9D reaction have been identified from these studies. First, compared to the quantitative generation of peroxoΔ9D with sodium dithionite, the rapid-mix experiments showed that reduced Fd is the catalytically competent electron donor for Δ9D. This implies an unanticipated role for reduced Fd that cannot be fulfilled by a chemical reductant. Second, the rate and yield was maximized with the ordered addition of acyl-ACP to resting Δ9D, then reduced Fd, and then O_2, which implies an ordered steady-state kinetic mechanism. This order provides an indication of how enzyme−substrate interactions may participate in gating the redox reactions and activation of O_2 for catalysis.

Figure 7 shows results of rapid-mix, chemical quench studies.[25] The reaction of the prereduced enzyme−substrate complex with O_2 gave a burst of product formation (open circles, Figure 7; $k_{burst} = k_7 = 95\ s^{-1}$) with a stoichiometry that suggested ~90% turnover of one

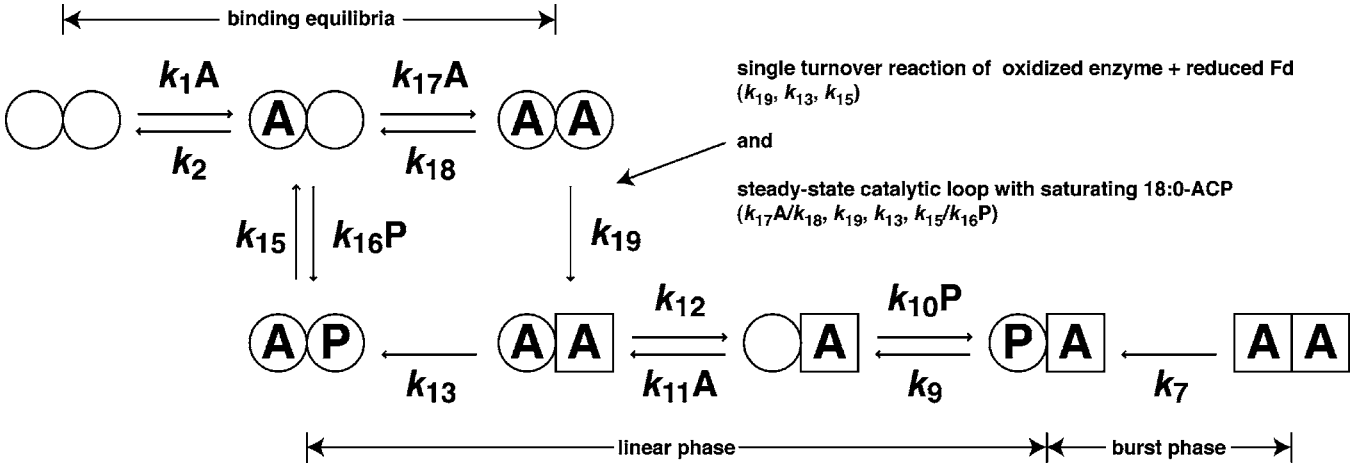

FIGURE 8. Kinetic model for dimeric Δ9D catalysis.[25] Circle symbols represent a Δ9D subunit containing a diferric center, and square symbols represent a Δ9D subunit containing a diferrous center. Bound substrate and product are indicated by A and P, respectively. Rate constants k_7 and k_{13} indicate irreversible reactions, k_9/k_{10}P and k_{15}/k_{16}P indicate reversible product binding, k_1A/k_2, k_{11}A/k_{12}, and k_{17}A/k_{18} indicate reversible substrate binding, and k_{19} indicates an assumed irreversible electron transfer from reduced Fd to diferric Δ9D.

subunit of the dimer. The burst was followed by a slower phase of product formation ($k_{linear} = 4.0\ s^{-1}$) with a yield consistent with turnover of the second subunit. For comparison, reaction of the oxidized enzyme−substrate complex with reduced Fd showed no prominent burst and gave a slower rate of product formation (solid circles, $k_{observed} = 3.4\ s^{-1}$). In this experiment, $k_{observed}$ was sufficient to allow ~1.5 turnovers before autoxidation of reduced Fd stopped the reaction. Analysis of deuterium isotope effects revealed only a modest effect on both k_{burst} ($^Dk_7 \approx 1.5$) and k_{linear} ($^Dk_{linear} \approx 1.4$), indicating that C−H bond cleavage does not contribute significantly to the rate-limiting steps of Δ9D catalysis.

Figure 8 shows a kinetic model for Δ9D catalysis.[25] This model includes (1) binding equilibria studied by fluorescence anisotropy, (2) burst and linear kinetics observed from reaction of the prereduced enzyme−substrate complex with O_2, (3) single-turnover reaction of the oxidized, substrate-saturated enzyme mixed with reduced Fd, and (4) steady-state catalysis.

Numerical integration and net rate analysis were used to evaluate this model.[25] It is important to note that numerical integration incorporated experimental results from each of the four types of experiments indicated above without a change in adjustable parameters other than initial concentrations and the time domain of reaction. Moreover, only a minimal set of unique rate constant values was required with equivalent rate constants assigned for similar reactions (e.g., chemical step(s), $k_7 = k_{13}$; product release, $k_9 = k_{15}$). The solid and dashed lines of Figure 7 show a close match between the calculated product formation rates and the experimental data from 10 to 1000 ms, including both the burst and linear reaction setups.

Net rate analysis[44] provided an important constraint to the validity of the kinetic model and the rate constant assignments. By this method, an explicit expression was written for V_{max} in the catalytic loop of Figure 8,[25] allowing predictive calculations using the values assigned for individual rate constants. For the model of Figure 8, the $V_{max} = k_{cat} \approx 1\ s^{-1}$ calculated per active site compared well to $k_{cat} \approx 0.5-0.7\ s^{-1}$ measured in steady state.[23,24,26] This close match provides substantial support for the validity of the proposed kinetic model.

The results of Figures 7 and 8 provide important insight into the Δ9D reaction. First, product release is likely to be rate-limiting since both types of rapid-mix reactions give single-turnover product accumulation faster than steady-state catalysis. This assessment is consistent with the accumulating evidence for substantial interactions between acyl-ACP and Δ9D. Second, the lack of a kinetic isotope effect indicates that reaction steps other than C−H bond cleavage are rate-limiting. If these steps occur prior to formation of diiron intermediates, it may not be possible to observe these as in other diiron enzymes.[45,46] This would represent a distinct aspect of the Δ9D reaction, which again may ultimately relate to the dominating influence of substrate-binding interactions throughout the Δ9D reaction.

Substrate Analogue Reactions

Substrate analogues have been used to investigate many enzyme reaction mechanisms. For Δ9D, this approach is complicated by the necessity of synthesizing the suitably modified acyl-ACPs and by active site constraints, which apparently limit the complexity of functional groups that can be bound. Nevertheless, our recent studies of acyl-ACP analogues have provided unique diagnostic information about the differential nature of reaction at the C-9 and C-10 positions. The determination of isotopic incorporation in the presence of either $^{18}O_2$ or $^{18}OH_2$ has also revealed details about the Δ9D mechanism within the paradigm of diiron enzyme reactivity.

Monounsaturated Acyl-ACPs. Positional isomers of monounsaturated 18:1-ACP were used to test active-site constraints and to investigate whether allylic rearrangement (and, by inference, substrate radical intermediates) might occur during catalysis.[47] Δ9D readily desaturated *trans*-Δ^7-18:1-ACP and *trans*-Δ^{11}-18:1-ACP but did not

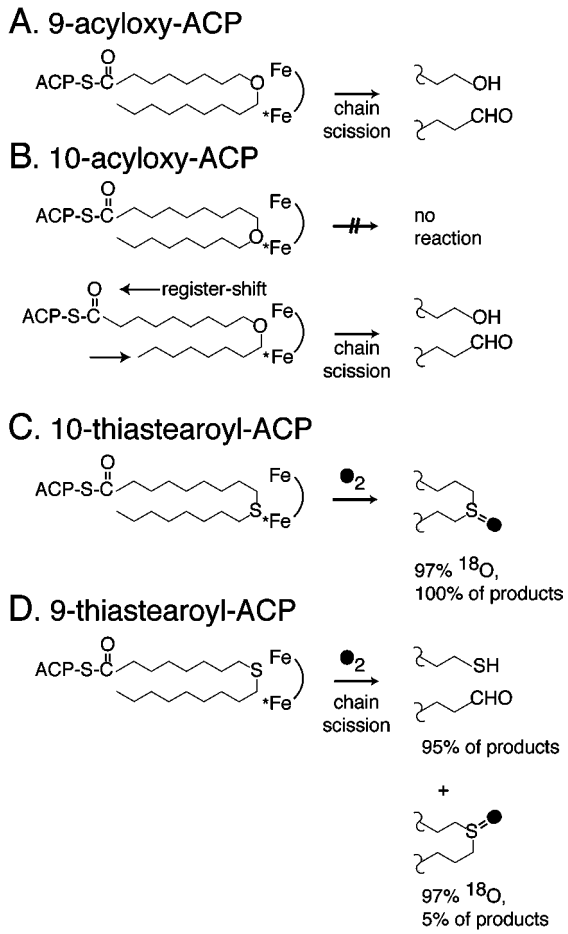

FIGURE 9. Register-shift and chain-scission reactions of Δ9D with acyl-ACP analogues: (A,B) acyloxy-ACPs;[48] (C,D) thiastearoyl-ACPs.[52] Heteroatom substitution at the site of reaction chemistry leads to alternative outcomes for desaturase reactions. Placement of an ether oxygen at the site of initial C−H bond cleavage blocks the reaction and causes a register shift of the substrate in the active site and chain scission at an adjacent carbon atom. Placement of a thiaether sulfur at the site of initial C−H bond cleavage permits high-fidelity transfer of an O-atom derived from O_2. Placement of either heteroatom adjacent to the site of initial C−H bond cleavage results in a quantitative chain-scission reaction.

react with either *trans*-Δ^9-18:1-ACP or any of the corresponding cis isomers. This selectivity is consistent with steric interactions exerting a strong influence on substrate binding. Thus acyl chains with restricted flexibility at the critical C-9 and C-10 positions are not suitable substrates for Δ9D.

Reaction of *trans*-Δ^{11}-18:1-ACP gave a single product, *cis*-Δ^9,*trans*-Δ^{11}-18:2-ACP. Notably, this product arose from reaction at C-9 and C-10 without interference from the *trans*-Δ^{11} bond, indicating proper binding of the substrate analogue *with the functional group past the diiron center*. In contrast, reaction of *trans*-Δ^7-18:1-ACP gave two products, *trans*-Δ^7,*cis*-Δ^9-18:2- (∼80%) and *trans*-Δ^7,*cis*-Δ^{10}-18:2-ACP (∼20%). The major product was again formed by reaction at C-9 and C-10 in a manner analogous to that observed with 18:0-ACP, while the minor product was assigned to arise from reaction of an alternative binding of *trans*-Δ^7-18:1 where C-10 and C-11 were arranged in the reactive configuration at the diiron oxidant (see Figure 4). In this case, the fatty acid would be bound in a shifted position in the active site. By assuming sufficient reactivity of the activated diiron center once these methylene groups were suitably positioned, all other aspects of the reaction could proceed to the formation of a cis double bond in an alternative position. This previously unknown introduction of a double bond in an alternative position was our first indication of "register shift", a mechanistically relevant misalignment of the acyl chain resulting in reaction at positions other than C-9 and C-10.

Acyloxy-ACPs. Fatty acyl analogues with an O-atom replacing a methylene group at the 8, 9, 10, or 11 positions of the acyl chain were next investigated (Figure 9A,B).[48] The experimental rationale was that placement of the ether oxygen would prevent oxidation at that position and thus force alternative reaction outcomes upon dissipation of the activated diiron center.

Reactions with either O-8 or O-11 acyloxy-ACPs gave a single product with a cis double bond between C-9 and C-10, corresponding to the same reaction specificity as the natural substrate. Moreover, the apparent kinetic parameters were also comparable. Thus an ether group adjacent to the site of reaction had no significant effect on reactivity. In contrast, reactions with both O-9 and O-10 acyloxy-ACPs reduced k_{cat} to ∼3% of 18:0-ACP and gave unique chemical outcomes. For O-9 acyloxy-ACP (Figure 9A), 8-hydroxyoctanoyl-ACP and 1-nonanal were the only products, corresponding to the anticipated binding register and an oxidative acyl chain cleavage between O-9 and C-10. In contrast, the O-10 substrate yielded 9-hydroxynonanoyl-ACP and 1-octanal as the only products (Figure 9B), corresponding to an obligate "register shift" of the acyloxy chain prior to acyl chain cleavage between O-10 and C-11. A number of oxidation mechanisms leading to an unstable hemiacetal are consistent with these products.[48]

The simplest interpretation of these results is that desaturation catalyzed by Δ9D initiates at C-10. In contrast, the integral membrane stearoyl-CoA Δ^9 desaturase catalyzes the same double bond insertion in a reaction initiated at C-9 as evidenced by kinetic isotope effect studies.[49,50] This represents a new mechanistic distinction between what have long been assumed to be functionally equivalent enzyme classes. The acyloxy-ACP results further suggest that a specific iron atom of the Δ9D diiron center may act as the leading oxidant in the desaturase reaction, as proposed for the reaction of Fe_A in ribonucleotide reductase with Tyr122.[16]

Thiastearoyl-ACPs. Thiastearates have been used to study the integral membrane desaturases. For example, after feeding thiastearates to *Saccharomyces cerevisiae* expressing membrane stearoyl-CoA desaturase, sulfoxides recovered from the culture medium showed a high enantiomeric excess[51] and a stereochemistry matching the observed H-atom removal.[49] This sulfoxidation reaction was designated "diverted" desaturation, the first demonstration of an alternative reaction outcome from what is

otherwise recognized to be a high-fidelity and high-specificity catalytic site.

We prepared 9- and 10-thiastearoyl-ACP analogues and reacted them with soluble Δ9D.[52] The goals were to determine whether the reactivity was the same as that for the integral membrane enzymes and to identify the origin of the O-atom incorporated into any putative sulfoxide products. Reaction of Δ9D with 10-thiastearoyl-ACP gave sulfoxidation only (Figure 9C) with the incorporated oxygen arising stoichiometrically from O_2. Surprisingly, however, the major outcome for reaction of Δ9D with 9-thiastearoyl-ACP was not sulfoxidation (Figure 9D) but was instead an acyl chain cleavage between S-9 and C-10, representing the second example of this result catalyzed by Δ9D with a heteroatom-substituted acyl chain. Single-turnover reactions with 9-thiastearoyl-ACP revealed that either sulfoxidation or acyl chain cleavage could occur from a single O_2 activation event. Thus it is likely that the products arise from partition between two alternative reactions of the thiastearoyl group bound within the enzyme active site. Furthermore, as with the acyloxy-ACPs, the pattern of thiastearoyl-ACP reactions implicates initiation of the Δ9D reaction at the 10-position.

The formation of isotopically labeled sulfoxides in the presence of $^{18}O_2$ demonstrates the Δ9D diiron center can catalyze O-atom transfer reactions *in the presence of an appropriate substrate analogue*. This implies participation of an activated electrophilic complex derived from the diiron center and O_2 in catalysis. The proven O-atom transfer capability also supports mechanistic linkages with other diiron enzymes; although it should be noted in closing that there is presently no evidence that a hydroxylated fatty acid serves as an intermediate in the normal desaturation reaction.

B.G.F. acknowledges generous funding from the National Institutes of Health (Grant GM-50853), the Searle Scholars Program, and the Shaw Scientist Program. K.S.L. was a Trainee of NIH Molecular Biophysics Training Grant T32 GM-08293. The authors also acknowledge the insightful efforts of our many outstanding collaborators.

References

(1) Sperling, P.; Ternes, P.; Zank, T. K.; Heinz, E. The evolution of desaturases. *Prostaglandins, Leukotrienes Essent. Fatty Acids* **2003**, *68*, 73−95.

(2) Fox, B. G. In *Comprehensive Biological Catalysis*; Sinnott, M., Ed.; Academic Press: London, 1998; Vol. 3, pp 261−348.

(3) Shanklin, J.; Cahoon, E. B. Desaturation and related modifications of fatty acids. *Annu. Rev. Plant Physiol. Plant Mol. Biol.* **1998**, *49*, 611−641.

(4) Funk, C. D. Prostaglandins and leukotrienes: advances in eicosanoid biology. *Science* **2001**, *294*, 1871−1875.

(5) Liechti, R.; Farmer, E. E. The jasmonate pathway. *Science* **2002**, *296*, 1649−1650.

(6) Kinney, A. J.; Cahoon, E. B.; Hitz, W. D. Manipulating desaturase activities in transgenic crop plants. *Biochem. Soc. Trans.* **2002**, *30*, 1099−1103.

(7) Broadwater, J. A.; Whittle, E.; Shanklin, J. Desaturation and hydroxylation: residues 148 and 324 of arabidopsis FAD2, in addition to substrate chain length, exert a major influence in partitioning of catalytic specificity. *J. Biol. Chem.* **2002**, *277*, 15613−15620.

(8) Reed, D. W.; Polichuk, D. R.; Buist, P. H.; Ambrose, S. J.; Sasata, R. J.; Savile, C. K.; Ross, A. R.; Covello, P. S. Mechanistic study of an improbable reaction: alkene dehydrogenation by the Δ12 acetylenase of *Crepis alpina*. *J. Am. Chem. Soc.* **2003**, *125*, 10635−10640.

(9) Shanklin, J.; Whittle, E.; Fox, B. G. Eight histidine residues are catalytically essential in a membrane associated iron enzyme, stearoyl-CoA desaturase, and are conserved in alkane hydroxylase and xylene monooxygenase. *Biochemistry* **1994**, *33*, 12787−12794.

(10) Behrouzian, B.; Buist, P. H. Mechanism of fatty acid desaturation: a bioorganic perspective. *Prostaglandins, Leukotrienes Essent. Fatty Acids* **2003**, *68*, 107−112.

(11) Ntambi, J. M.; Miyazaki, M.; Stoehr, J. P.; Lan, H.; Kendziorski, C. M.; Yandell, B. S.; Song, Y.; Cohen, P.; Friedman, J. M.; Attie, A. D. Loss of stearoyl-CoA desaturase-1 function protects mice against adiposity. *Proc. Natl. Acad. Sci. U.S.A.* **2002**, *99*, 11482−11486.

(12) Fox, B. G.; Shanklin, J.; Ai, J.; Loehr, T. M.; Sanders-Loehr, J. Resonance Raman evidence for an Fe−O−Fe center in stearoyl-ACP desaturase. Primary sequence identity with other diiron-oxo proteins. *Biochemistry* **1994**, *33*, 12776−12786.

(13) Nordlund, P.; Eklund, H. Di-iron−carboxylate proteins. *Curr. Opin. Struct. Biol.* **1995**, *5*, 758−766.

(14) Wallar, B. J.; Lipscomb, J. D. Dioxygen activation by enzymes containing binuclear non-heme iron clusters. *Chem. Rev.* **1996**, *96*, 2625−2657.

(15) Sahlin, M.; Sjöberg, B. M. Ribonucleotide reductase. A virtual playground for electron-transfer reactions. *Subcell. Biochem.* **2000**, *35*, 405−443.

(16) Nordlund, P.; Eklund, H. Structure and function of the *Escherichia coli* ribonucleotide reductase protein R2. *J. Mol. Biol.* **1993**, *232*, 123−164.

(17) Lindqvist, Y.; Huang, W.; Schneider, G.; Shanklin, J. Crystal structure of Δ9 stearoyl-acyl carrier protein desaturase from castor seed and its relationship to other diiron proteins. *EMBO J.* **1996**, *15*, 4081−4092.

(18) Solomon, E. I.; Brunold, T. C.; Davis, M. I.; Kemsley, J. N.; Lee, S.-K.; Lehnert, N.; Neese, F.; Skulan, A. J.; Yang, Y.-S.; Zhou, J. Geometric and electronic structure/function correlations in non-heme iron enzymes. *Chem. Rev.* **2000**, *100*, 235−349.

(19) Merkx, M.; Kopp, D. A.; Sazinsky, M. H.; Blazyk, J. L.; Muller, J.; Lippard, S. J. Dioxygen activation and methane hydroxylation by soluble methane monooxygenase: A tale of two irons and three proteins. *Angew. Chem., Int. Ed.* **2001**, *40*, 2782−2807.

(20) Mitchell, K. H.; Fox, B. G. In *Manual of Environmental Microbiology Section VIII Biotransformation and Biodegradation*, 2nd ed.; Hurst, C. J., Crawford, R. L., Knudsen, G. R., McInerney, M. J., Stetzenbach, L. D., Eds.; ASM Press: Washington, DC, 2001; pp 997−1007.

(21) Haas, J. A.; Frederick, M. A.; Fox, B. G. Chemical and posttranslational modification of *Escherichia coli* acyl carrier protein for preparation of dansyl-acyl carrier proteins. *Protein Expression Purif.* **2000**, *20*, 274−284.

(22) Shanklin, J. Overexpression and purification of the *Escherichia coli* inner membrane enzyme acyl-acyl carrier protein synthase in an active form. *Protein Expression Purif.* **2000**, *18*, 355−360.

(23) Broadwater, J. A.; Ai, J.; Loehr, T. M.; Sanders-Loehr, J.; Fox, B. G. Peroxodiferric intermediate of stearoyl-acyl carrier protein Δ^9 desaturase: Oxidase reactivity during single turnover and implications for the mechanism of desaturation. *Biochemistry* **1998**, *37*, 14664−14671.

(24) Haas, J. A.; Fox, B. G. The role of hydrophobic partitioning in substrate selectivity and turnover of the *Ricinus communis* stearoyl-ACP Δ^9 desaturase. *Biochemistry* **1999**, *38*, 12833−12840.

(25) Lyle, K. S.; Haas, J. A.; Fox, B. G. Rapid-mix and chemical quench studies of ferredoxin-reduced stearoyl-acyl carrier protein desaturase. *Biochemistry* **2003**, *42*, 5857−5866.

(26) Whittle, E.; Shanklin, J. Engineering delta 9-16:0-acyl carrier protein (ACP) desaturase specificity based on combinatorial saturation mutagenesis and logical redesign of the castor delta 9-18:0-ACP desaturase. *J. Biol. Chem.* **2001**, *276*, 21500−21505.

(27) Voegtli, W. C.; Khidekel, N.; Baldwin, J.; Ley, B. A.; Bollinger, J. M., Jr.; Rosenzweig, A. C. Crystal structure of the ribonucleotide reductase R2 mutant that accumulates a μ-1,2-peroxodiiron(III) intermediate during oxygen activation. *J. Am. Chem. Soc.* **2000**, *122*, 3255−3261.

(28) Canada, K. A.; Iwashita, S.; Shim, H.; Wood, T. K. Directed evolution of toluene ortho-monooxygenase for enhanced 1-naphthol synthesis and chlorinated ethene degradation. *J. Bacteriol.* **2002**, *184*, 344−349.

(29) Mitchell, K. H.; Studts, J. M.; Fox, B. G. Combined participation of effector protein binding and hydroxylase active site residues provide toluene 4-monooxygenase regiospecificity. *Biochemistry* **2002**, *41*, 3176−3188.
(30) Lakowicz, J. R. *Principles of Fluorescence Spectroscopy*, 2nd ed.; Kluwer Academic/Plenum Publishers: New York, 1999.
(31) Haas, J. A.; Fox, B. G. Fluorescence anisotropy studies of enzyme−substrate complex formation in stearoyl-ACP desaturase. *Biochemistry* **2002**, *41*, 14472−14481.
(32) Bruice, T. C.; Benkovic, S. J. Chemical basis for enzyme catalysis. *Biochemistry* **2000**, *39*, 6267−6274.
(33) Behrouzian, B.; Savile, C. K.; Dawson, B.; Buist, P. H.; Shanklin, J. Exploring the hydroxylation−dehydrogenation connection: novel catalytic activity of castor stearoyl-ACP Δ^9 desaturase. *J. Am. Chem. Soc.* **2002**, *124*, 3277−3283.
(34) Fox, B. G.; Shanklin, J.; Somerville, C.; Münck, E. Stearoyl acyl carrier protein Δ^9 desaturase from *Ricinus communis* is a diiron-oxo protein. *Proc. Natl. Acad. Sci. U.S.A.* **1993**, *90*, 2486−2490.
(35) Shu, L.; Broadwater, J. A.; Achim, C.; Fox, B. G.; Münck, E.; Que, L., Jr. EXAFS and Mössbauer characterization of the diiron(III) site in stearoyl-acyl-carrier-protein (ACP) Δ^9 desaturase. *J. Biol. Inorg. Chem.* **1998**, *3*, 392−400.
(36) Broadwater, J. A.; Achim, C.; Münck, E.; Fox, B. G. Mössbauer studies of the formation and reactivity of a quasi-stable peroxodiferric intermediate of stearoyl-acyl carrier protein Δ^9 desaturase. *Biochemistry* **1999**, *38*, 12197−12204.
(37) Yang, Y.-S.; Broadwater, J. A.; Fox, B. G.; Solomon, E. I. Circular dichroism and magnetic circular dichroism studies of the reduced binuclear non-heme stearoyl-ACP Δ^9 desaturase: Substrate binding and comparison to ribonucleotide reductase. *J. Am. Chem. Soc.* **1999**, *121*, 2770−2783.
(38) Brunold, T. C.; Tamura, N.; Kitajima, N.; Moro-oka, Y.; Solomon, E. I. Spectroscopic study of $[Fe(O_2))(OBz)_2\{HB(pz')_3\}_2]$: Nature of the μ-1,2 peroxide-Fe(III) bond and its possible relevance to O_2 activation by non-heme iron enzymes. *J. Am. Chem. Soc.* **1998**, *120*, 5674−5690.
(39) Lee, S.-K.; Fox, B. G.; Froland, W. F.; Lipscomb, J. D.; Münck, E. A transient intermediate of the methane monooxygenase catalytic cycle containing an $Fe^{IV}Fe^{IV}$ cluster. *J. Am. Chem. Soc.* **1993**, *115*, 6450−6451.
(40) Lyle, K. S.; Ai, J.; Moenne-Loccoz, P.; Sanders-Loehr, J.; Loehr, T. M.; Fox, B. G. Resonance Raman studies of the stoichiometric catalytic turnover of a substrate-stearoyl-acyl carrier protein Δ^9 desaturase complex. *Biochemistry* **2000**, *39*, 10507−10513.
(41) Ling, J.; Sahlin, M.; Sjöberg, B.-M.; Loehr, T. M.; Sanders-Loehr, J. Dioxygen is the source of the oxo bridge in ribonucleotide reductase. *J. Biol. Chem.* **1994**, *269*, 5596−5601.
(42) Burdi, D.; Willems, J.-P.; Riggs-Gelasco, P.; Antholine, W. E.; Stubbe, J.; Hoffman, B. M. The core structure of X generated in the assembly of the diiron cluster of ribonucleotide reductase: $^{17}O_2$ and $H_2{}^{17}O$ ENDOR. *J. Am. Chem. Soc.* **1998**, *120*, 12910−12919.
(43) Ruzicka, F.; Huang, D.-S.; Donnelly, M. I.; Frey, P. A. Methane monooxygenase catalyzed oxidation of 1,1-dimethylcyclopropane. Evidence for radical and carbocationic intermediates. *Biochemistry* **1990**, *29*, 1696−1700.
(44) Cleland, W. W. Partition analysis and the concept of net rate constant as tools in enzyme kinetics. *Biochemistry* **1975**, *14*, 3220−3224.
(45) Lee, S.-K.; Nesheim, J. C.; Lipscomb, J. D. Transient intermediates of the methane monooxygenase catalytic cycle. *J. Biol. Chem.* **1993**, *268*, 21569−21577.
(46) Bollinger, J. M., Jr.; Edmondson, D. E.; Huynh, B. H.; Filley, J.; Norton, J. R.; Stubbe, J. Mechanism of assembly of the tyrosyl radical dinuclear iron cluster cofactor of ribonucleotide reductase. *Science* **1991**, *253*, 292−298.
(47) Broadwater, J. A.; Laundre, B.; Fox, B. G. Desaturation of *trans*-octadecenoyl-acyl carrier protein by stearoyl-acyl carrier protein Δ^9 desaturase. *J. Inorg. Biochem.* **2000**, *78*, 7−14.
(48) Rogge, C. E.; Fox, B. G. Desaturation, chain scission, and register-shift of oxygen-substituted fatty acids during reaction with stearoyl-ACP desaturase. *Biochemistry* **2002**, *41*, 10141−10148.
(49) Schroepfer, G. J., Jr.; Bloch, K. The stereospecific conversion of stearic acid to oleic acid. *J. Biol. Chem.* **1965**, *240*, 54−63.
(50) Buist, P. H.; Behrouzian, B. Use of deuterium kinetic isotope effects to probe the cryptoregiospecificity of Δ^9 desaturation. *J. Am. Chem. Soc.* **1996**, *118*, 6295−6296.
(51) Buist, P. H.; Marecak, D. M. Stereochemical analysis of sulfoxides obtained by diverted desaturation. *J. Am. Chem. Soc.* **1992**, *114*, 5073−5080.
(52) White, R. D.; Fox, B. G. Chain cleavage and sulfoxidation of thiastearoyl-ACP upon reaction with stearoyl-ACP desaturase. *Biochemistry* **2003**, *42*, 7828−7835.

AR030186H